MOLECULAR IMAGING AND BIOLOGY

Mol Imaging Biol (2019) 21:696–704
DOI: 10.1007/s11307-018-1286-8

Published Online: 30 October 2018

RESEARCH ARTICLE

Development of a Fluorinated Analogue of Erlotinib for PET Imaging of EGFR Mutation–Positive NSCLC

Ofer Shamni, Hilbert Grievink, Batel Itamar, Eyal Mishani, Galith Abourbeh

Cyclotron/Radiochemistry/MicroPET Unit, Hadassah Hebrew University Hospital, Hadassah Medical Organization, 91120, Jerusalem, Israel

Abstract

Purpose: Positron emission tomography (PET) using [^{11}C]erlotinib identifies non-small cell lung carcinoma (NSCLC) tumors with activating mutations in the epidermal growth factor receptor ($EGFR_m$). The short half-life of C-11, however, limits its clinical utility to centers with a nearby cyclotron. We therefore developed a F-18–labeled analogue of erlotinib for imaging $EGFR_m$ NSCLC.

Procedures: 6-O-Fluoroethylerlotinib (6-O-FEE) was synthesized and its anti-proliferative activity was tested using human NSCLC cell lines. The F-18–labeled compound, 6-O-[^{18}F]FEE, was obtained in a two-step synthesis, and PET acquisitions were carried out following its injection to NSCLC tumor–bearing mice.

Results: In vitro, 6-O-FEE had maintained the selectivity and potency of erlotinib to $EGFR_m$ NSCLC. *In vivo*, 6-O-[^{18}F]FEE accumulation in $EGFR_m$ tumors at 60 min after injection was 2- and 3.3-fold higher than in erlotinib-resistant or erlotinib-insensitive tumors, respectively.

Conclusions: 6-O-[^{18}F]FEE holds promise for imaging $EGFR_m$ NSCLC, warranting further investigation to fully explore its potential for stratifying NSCLC patients.

Key words: EGFR, NSCLC, Imaging, PET, Erlotinib, Fluorine-18, 6-O-[^{18}F]FEE, TKI

Introduction

The epidermal growth factor receptor (EGFR) is overexpressed in over 60 % of non-small cell lung carcinoma (NSCLC) tumors, and its mutational status in advanced/ metastatic NSCLC has both a prognostic value and a therapeutic impact [1–5]. The predominant activating mutations in this receptor, *i.e.*, exon 19 deletions and the L858R point mutation in exon 21, are associated with responsiveness to EGFR tyrosine kinase inhibitors (TKIs) [6, 7]. These sensitizing mutations are found in 10–15 % of Caucasian patients with NSCLC and in up to 50 % of Asian patients [6–9].

To date, optimal first-line treatment of EGFR mutation–positive ($EGFR_m$) NSCLC comprises any of the approved EGFR TKIs, including gefitinib, erlotinib, and afatinib [6, 7, 10, 11]. Recently, the third-generation EGFR TKI, osimertinib, has also been approved for the first-line treatment of $EGFR_m$ NSCLC [12]. These EGFR TKIs offer a longer progression-free survival (PFS), higher response rate (RR), and reduced side effects, compared to standard chemotherapy [6, 7]. Conversely, NSCLC patients whose tumors do not harbor sensitizing EGFR mutations do not benefit from EGFR TKI therapy and should be treated with chemotherapy, specific inhibitors of other oncoproteins, or immune checkpoint inhibitors [6, 10, 11, 13]. Since

Electronic supplementary material The online version of this article (https://doi.org/10.1007/s11307-018-1286-8) contains supplementary material, which is available to authorized users.

Correspondence to: Galith Abourbeh; *e-mail:* abourbehg@hadassah.org.il

activating EGFR mutations are present in only a subset of NSCLC patients, current indications recommend that the mutational status of this receptor is examined prior to therapy [6, 7, 10, 14].

Typically, EGFR mutation testing in NSCLC is carried out using tumor tissue biopsies or fine-needle aspirates, which entail invasive procedures and provide no information regarding the presence of distant metastases and/or their molecular characteristics [5, 7]. Additionally, EGFR mutation analysis using tissue/cytology specimens is not always feasible, often due to suboptimal tumor DNA quantity and/or quality for genomic characterization [6–8, 15, 16]. Consequently, different non-invasive approaches which provide systemic information have been explored for obtaining molecular information concerning the EGFR's mutational status in NSCLC patients, including liquid biopsies [4, 17, 18], analysis of computed tomography–based radiomic features [19], and the use of radiolabeled TKIs for positron emission tomography (PET) molecular imaging (MI) [20–23].

In this regard, the use of [^{11}C]erlotinib-PET for detecting $EGFR_m$ NSCLC and metastases has been reported both in animal models and in human subjects [17, 20, 24–32], offering a non-invasive and sensitive tool for assessing the mutational status of the EGFR. Nonetheless, the relatively short half-life of C-11 (~20 min) poses a challenge to the wider clinical application of [^{11}C]erlotinib-PET, since it limits its use to centers with a nearby cyclotron, calling for the research and development of novel EGFR TK PET probes which are labeled with longer-lived isotopes, such as F-18 [22].

To extend the clinical impact of erlotinib-PET for detecting $EGFR_m$ NSCLCs, we have designed, synthetized, and labeled with F-18 the erlotinib analogue, 6-O-fluoroethylerlotinib (6-O-FEE) (Fig. 1). The synthesis and anti-proliferative effect of 6-O-FEE in human NSCLC cell lines, as well as the stability of 6-O-[^{18}F]FEE *in vivo* and its ability to identify $EGFR_m$ NSCLC in tumor-bearing mice, are described herein.

Materials and Methods

General

Insulin, transferrin, HEPES, and sodium pyruvate were purchased from Biological Industries (BI) (Kibbutz Beit Haemek, Israel). Sodium selenite, hydrocortisone, ethanolamine, O-phosphorylethanolamine, 3,3′,5-Triiodo-L-thyronine (T_3), bovine serum albumin (BSA), and *N*,*N*-dimethylformamide (DMF) were purchased from Sigma-Aldrich (Rehovot, Israel). Captisol® was obtained from CyDex Pharmaceuticals Inc. (KS, USA).

Hsd: Athymic Nude-Fox1nu mice (male, 4–5 weeks) and BALB/c olaHsd mice (male, 9–10 weeks) were obtained from Envigo (Rehovot, Israel). All animal studies were conducted under protocol number MD-13-13833-5, approved by the Animal Research Ethics Committee of the Hebrew University of Jerusalem, and in accordance with its guidelines. Animals were acclimated for at least 3 days prior to their inoculation with tumor cells. Animals were routinely kept in 12-h light/dark cycles and provided with food and water *ad libitum*.

Instrumentation

See the description in the electronic supplementary material (ESM).

Synthesis of 6-O-Fluoroethylerlotinib (6-O-FEE) Standard

See the description in the ESM.

Synthesis of 6-O-[^{18}F]Fluoroethylerlotinib (6-O-[^{18}F]FEE)

[^{18}F]Fluoride ion was produced by the ^{18}O(p,n) ^{18}F nuclear reaction using 3 ml enriched [^{18}O]water (98 % isotopic purity, Rotem Industries, Mishor Yamin, Israel) as a target and an IBA 18/9 cyclotron. Thereafter, [^{18}F]F^-/[^{18}O]H_2O was transferred to the module, loaded onto an anion exchange column (30PS-HCO_3, Macherey Nagel, Düren, Germany), and eluted with 0.5 ml of K_2CO_3 solution (8 mg/ml) to the reaction vessel. After addition of Kryptofix-2.2.2 (15 mg dissolved in 1 ml MeCN, Merck, Darmstadt, Germany), azeotropic removal of water and MeCN was achieved by heating the reactor to 82 °C under a stream of argon (2.4 bar) and reduced pressure for 2 min, yielding a pressure of 0.2 bar inside the reactor. This was

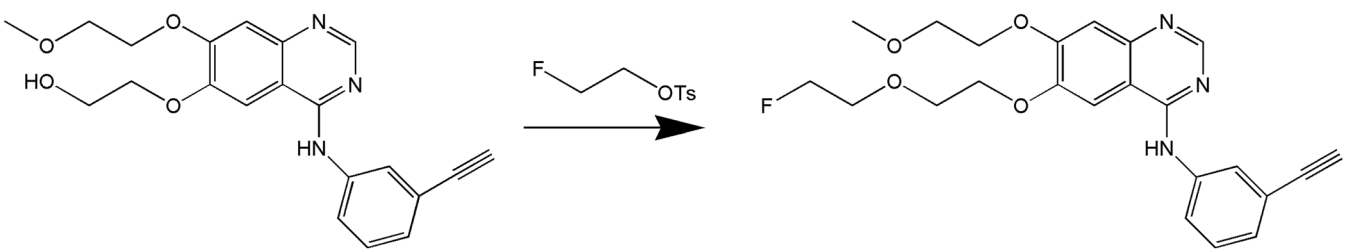

Fig. 1. Synthesis of 6-O-fluoroethylerlotinib (6-O-FEE) reference standard.

followed by an additional 3.5 min under 102 °C and reduced pressure, to yield a pressure of 0.04 bar inside the reactor.

Reagent vials were loaded onto the GE TRACER Lab Fx_{FN} module as follows: vial 1 (V1), potassium carbonate (0.5 ml of a 8 mg/ml solution, Sigma-Aldrich); V2, Kryptofix-2.2.2 (15 mg dissolved in 1 ml MeCN); V3, 11–13 mg ethylene 1,2-bis(tosylate) dissolved in 0.75 ml dry MeCN; V4, 1 ml of MeCN; V7, 1.8 ml of ethanol; V8, 4 ml of H_2O (HPLC grade); SPE vial, 24 ml of HPLC water; and collection vial, 12 ml of 0.9 % sodium chloride solution for injection. The Fx-FDOPA module was prepared as follows: V1, desmethylerlotinib (11 mg) dissolved in 0.6 ml dry DMF; V2, 1.5 ml of acetate buffer (0.1 M, pH 3.8; MeCN (6:4)) and 3 mg of NaH, directly added to the reactor and flushed with argon.

6-O-[^{18}F]Fluoroethylerlotinib was obtained in a fully automated two-step synthesis, as depicted in Fig. 2, using an automated GE TRACER Lab Fx_{FN} module coupled to a Fx-FDOPA module (Suppl. Figs. 1 and 2; see ESM). In the first step, [^{18}F]fluoroethyltosylate was obtained from ethylene 1,2-bis(tosylate), as previously published [33], and in the second step, it was further reacted with desmethylerlotinib to yield the desired product. In brief, a solution of ethylene 1,2-bis(tosylate) (ABX, Radeberg, Germany, 11–13 mg) dissolved in anhydrous MeCN (750 µl) was added to dried [^{18}F]fluoride. The reaction vessel was heated to 120 °C while stirring for 10 min and thereafter cooled to 50 °C. The ensuing [^{18}F]fluoroethyltosylate was further diluted with 1 ml MeCN, filtered, and transferred to a second reactor (Fx-FDOPA module) that was pre-stirred and heated under argon stream for 5 min at 40 °C, containing 11 mg of 6-O-desmethylerlotinib dissolved in 0.6 ml of DMF and 3–4 mg of NaH. The combined reaction mixture was then heated to 90 °C and stirred for 10 min in a sealed reactor, cooled to 60 °C and diluted with 1.5 ml of acetate buffer (0.1 M, pH 3.8; MeCN (6:4)). The crude solution was then filtered and purified on a semi-preparative C18 column (5 µm, 10 mm × 250 mm, Luna, Phenomenex, Torrance, CA, USA), equipped with a UV detector operated at 254 nm and a radio-detector, using the aforementioned acetate buffer (MeCN) as eluent, at a flow rate of 4 ml/min. The final product (retention time at 14 min) was collected in a solid-phase extraction vial and was further diluted with 24 ml of water (HPLC grade). The obtained solution was then loaded onto a C18-Plus Sep-Pak cartridge (Waters Corporation, Milford, MA, USA), pre-activated with 5 ml ethanol and 10 ml of water (HPLC grade), and washed with an additional 4 ml of water. The product was subsequently eluted using 1.8 ml ethanol and was further diluted with 18.2 ml of isotonic saline.

Quality Control Analysis of 6-O-[^{18}F]FEE

See the description in the ESM.

Cell Culture

See the description in the ESM.

Inhibition of Cell Growth

QG56 (3000 cells), HCC827, NCI-H3255 (5000 cells), and NCI-H1975 (7000 cells) were seeded and cultured in 96-well plates. Twenty-four to 48 h after seeding, cells were treated with increasing concentrations (0–100 µM) of erlotinib (Cayman Chemical, Ann Arbor, MI, USA) or 6-O-FEE. The media containing the inhibitors (0.05 % DMSO, 0.1 % ethanol) were freshly prepared and replaced every 24 h. Following 72 h of treatment, cell growth was determined by methylene blue assay [34]. The median inhibitory concentrations (IC_{50}) for cell growth of each cell line were calculated using GraphPad Prism 5.0 software. Experiments were repeated three to four times for each cell line, with three to six replicates per tested concentration.

NSCLC Xenografts

Mice were anesthetized with isoflurane (1–2 % in oxygen) and injected subcutaneously (s.c.) in the right front flank with a suspension of five million cells in medium containing Matrigel (BD Biosciences, Beit Haemek, Israel, 20 % (*v*/*v*)).

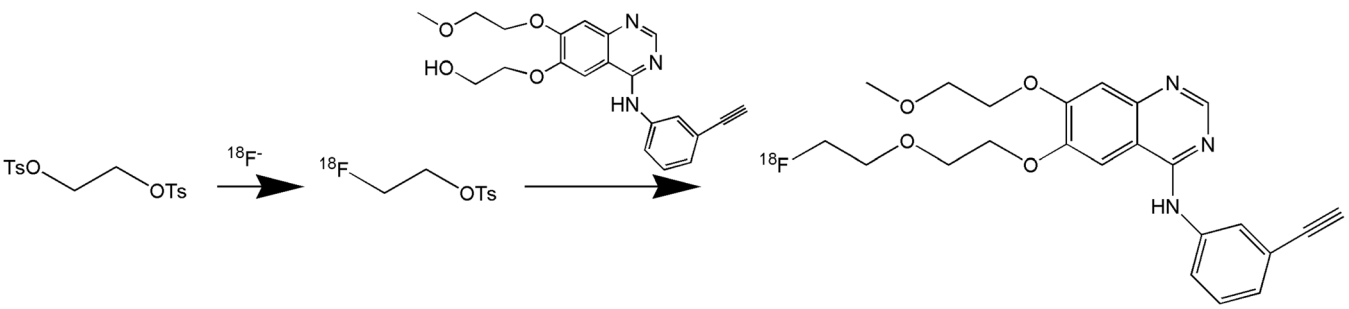

Fig. 2. Two-step radiosynthesis of 6-O-[^{18}F]FEE.

MicroPET/CT Studies

Three weeks after inoculation of cells, tumor-bearing mice (32.3 g ($n = 38$)) were anesthetized with isoflurane and kept at 38 °C using a heating pad. After performing a CT attenuation-correction scan, PET acquisitions were carried out using an Inveon™ MM PET-CT scanner (Siemens Medical Solutions, USA). One-hour PET acquisitions were started simultaneously to 6-O-[^{18}F]FEE injection *via* the lateral tail-vein (6.8 ± 1.0 MBq ($n = 38$)). Subsequently, mice were maintained in the same position and injected i.v. with 2-deoxy-2-[^{18}F]fluoro-D-glucose ([^{18}F]FDG, 6.7 ± 1.0 MBq ($n = 31$)). Forty minutes later, a second 20-min PET acquisition was performed. Blocking studies (carrier-added) were carried out in HCC827 ($n = 9$) and NCI-H1975 ($n = 6$) tumor–bearing mice, wherein erlotinib hydrochloride (OSI-744, Selleck Chemicals) dissolved in 20 % Captisol® was injected at a dose equivalent to 6.4 ± 0.4 mg/kg erlotinib, 3–10 min prior to the injection of 6-O-[^{18}F]FEE.

Image processing and reconstruction were carried out as previously described [20]. Tumors' volumes of interest (VOIs) were delineated manually, based on the fused PET (6-O-[^{18}F]FEE or [^{18}F]FDG) and CT images, and the corresponding 6-O-[^{18}F]FEE time-activity curves (TACs) were generated. Distribution of radioactivity was calculated and expressed in standardized uptake values (SUVs) as previously described [20].

In Vivo Stability Assay

See the description in the ESM.

Statistics

Statistical analysis was made using GraphPad Prism 5 software. Unless otherwise stated, data is expressed as mean ± SD. Median inhibitory concentration (IC_{50}) values of 6-O-FEE and erlotinib for cell growth inhibition of each cell line were compared using Student's *t* test. Comparisons of 6-O-[^{18}F]FEE uptake in tumors, in imaging studies, were made using one-way ANOVA, followed by *Dunnett's* post hoc test, using HCC827 tumor–bearing mice as the control group. The level of significance was regularly set at $p < 0.05$.

Results

Synthesis of 6-O-Fluoroethylerlotinib Standard and 6-O-[^{18}F]Fluoroethylerlotinib

6-O-FEE was obtained with 32.3 % yield (23 mg) and a purity higher than 99 %, as determined by analytical HPLC. The overall synthesis time of 6-O-[^{18}F]FEE from the end of bombardment (EOB) was 110 min, including purification and formulation (9 % ethanol in saline). An average radioactivity of 10.9 ± 5.6 GBq ($n = 8$) was obtained, with an average radiochemical yield of 5.7 ± 3.2 % and a mean molar activity of 146 ± 49 GBq/μmol, all decay-corrected (DC) to the EOB. Radiochemical purity was routinely greater than 99 %. Identification of 6-O-[^{18}F]FEE was confirmed by a co-injection of unlabeled 6-O-FEE to the HPLC, having retention times of 10.6–10.9 min. The stability of 6-O-[^{18}F]FEE in solution at room temperature was examined hourly for 4 h using radio-TLC and HPLC, and the compound remained stable throughout the examination period (Suppl. Fig. 3, ESM).

Growth Inhibition of NSCLC Cell Lines In Vitro

The anti-proliferative effects of 6-O-FEE and erlotinib were tested *in vitro* using four human NSCLC cell lines that harbor the prevailing EGFR variants identified in NSCLC patients. The IC_{50} values presented in Table 1 indicate that erlotinib and 6-O-FEE exhibited comparable potencies and selectivities towards $EGFR_m$ cell lines. Though the IC_{50} value of 6-O-FEE towards HCC827 cells was almost tenfold higher than that of erlotinib, the difference was not statistically significant, and both compounds demonstrated high inhibitory potencies towards this cell line, in the low (1–9) nM range. Both erlotinib and 6-O-FEE had IC_{50} values 2–3 orders of magnitude higher with respect to the TKI-resistant (NCI-H1975) and the TKI-insensitive (QG56) cell lines, compared to the TKI-sensitive (NCI-H3255 and HCC827) cells.

Imaging NSCLC Tumor–Bearing Mice Using 6-O-[^{18}F]FEE

The kinetics of radioactivity distribution was examined for 1 h following i.v. injection 6-O-[^{18}F]FEE to NSCLC tumor–bearing mice. The TACs presented in Fig. 3 demonstrate two to threefold higher radioactivity concentrations in HCC827 tumors, compared to those in NCI-H1975 and QG56 tumors, with mean SUVs of 1.0, 0.5, and 0.3, respectively, at 60 min after injection. Moreover, following its initial accumulation in the tumor tissue, the radioactivity was retained in HCC827 and NCI-H1975 tumors, whereas a slow decline in radioactivity concentration was measured in QG56 tumors.

To investigate whether the accumulation of radioactivity in HCC827 and NCI-H1975 tumors was specific, erlotinib was administered in excess (6.4 ± 0.4 mg/kg) 3–10 min prior to 6-O-[^{18}F]FEE injection to tumor-bearing mice. As depicted in Fig. 4, pre-administration of erlotinib had resulted in an almost twofold reduction in HCC827 tumor uptake at 60 min after 6-O-[^{18}F]FEE injection (mean SUVs of 1.04 and 0.55), albeit the difference was not statistically significant. In contrast to the reduced radioactivity uptake measured in HCC827 tumors after pre-administration of erlotinib in excess, radioactivity concentrations in NCI-H1975 tumors had in fact increased after pre-injection of

Table 1.. Anti-proliferative effect of 6-O-FEE and erlotinib in human NSCLC cell cultures

Cell line	Type of EGFR mutation	IC_{50} of erlotinib [μM] (*n*)	IC_{50} of 6-O-FEE [μM] (*n*)
QG56	None (wt EGFR)	12.6 ± 5.7 (4)	14.4 ± 4.6 (3)
HCC827	Activating (delE746-A750)	0.001 ± 0.001 (3)	0.009 ± 0.009 (4)
NCI-H3255	Activating (L858R point mutation)	0.05 ± 0.03 (3)	0.03 ± 0.04 (3)
NCI-H1975	Double (L858R + T790M)	3.2 ± 1.1 (3)	3.6 ± 1.5 (3)

non-labeled erlotinib, from a mean SUV of 0.5 to 0.7 at 60 min after 6-O-[^{18}F]FEE injection (Fig. 4).

Representative PET-CT slice images following 6-O-[^{18}F]FEE injection are illustrated in Fig. 5. Similar to the results obtained with [^{11}C]erlotinib [20, 35], the predominant route of 6-O-[^{18}F]FEE elimination was *via* hepatobiliary clearance.

In Vivo Stability

The metabolic fate of 6-O-[^{18}F]FEE was studied 2, 15, and 30 min after its injection to BALB/c mice. To this end, mice were sacrificed at the allotted time points after injection, followed by collection of blood and urine samples and excision of the entire liver. The percentages of extracted radioactivity from the blood and the liver at each time point are illustrated in Fig. 6a, revealing consistent levels of 49 ± 14 % and 84 ± 2 % extraction from the blood and the liver, respectively, at the three studied time points. To evaluate the fraction of extracted radioactivity which could be attributed to 6-O-[^{18}F]FEE, the processed plasma, liver, and urine samples were loaded onto normal-phase TLC plates, and the radioactive bands were visualized using a phosphor screen. The radio-TLC plates presented in Fig. 6b indicate that over 96 % of the radioactivity present in plasma at all three time points represented the intact compound. Radioactive metabolites in liver samples could be detected already at 2 min, representing about 2 % of the extracted radioactivity. At later time points, the fraction of radioactive metabolites had further increased, and 6-O-[^{18}F]FEE represented 80–85 % of the extracted radioactivity in the liver. The presence of radioactive metabolites in urine sample could also be detected, although faintly, already at 2 min after injection. Several polar metabolites were apparent at the later time points, accounting for essentially all the radioactive signal in the urine.

Discussion

We have designed, synthetized, and investigated the fluorinated analogue of erlotinib, 6-O-FEE (Fig. 1). *In vitro* experiments using human NSCLC cell cultures indicated that similar to erlotinib, 6-O-FEE was 2–3 orders of magnitude more potent in inhibiting the proliferation of $EGFR_m$ cells (HCC827 and NCI-H3255) compared to those expressing the acquired T790M resistance mutation (NCI-H1975) or the wild-type (wt) receptor (QG56) (Table 1), suggesting that this analogue had maintained the increased affinity of erlotinib to the predominant sensitizing mutations of the EGFR [36].

Subsequently, 6-O-FEE was labeled with fluorine-18 *via* a two-step synthesis (Fig. 2) and administered to NSCLC tumor–bearing mice with or without pre-injection of erlotinib in excess. The tumor TACs obtained following injection of 6-O-[^{18}F]FEE revealed 2- and 3.3-fold higher accumulation of radioactivity in HCC827 compared to NCI-H1975 and QG56 tumors, with mean SUVs of 1.0, 0.5, and 0.3, respectively, at 60 min after injection (Fig. 3). These results are in good agreement with those previously obtained with [^{11}C]erlotinib, wherein a 3.5-fold higher accumulation of radioactivity was

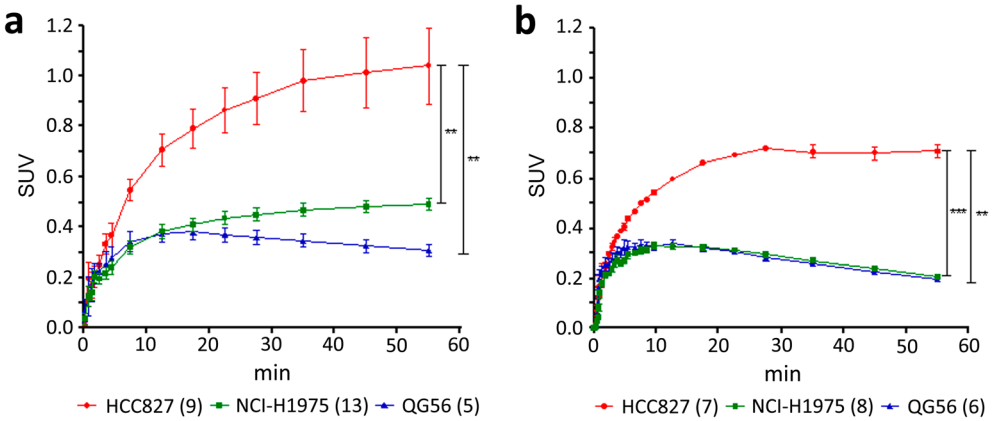

Fig. 3. Time-activity curves of **a** 6-O-[^{18}F]FEE and **b** [^{11}C]erlotinib following their i.v. injection to NSCLC tumor–bearing mice. Results are presented as mean ± SEM, and the number of animals per group is listed in brackets. $^{**}p < 0.01$; $^{***}p < 0.001$.

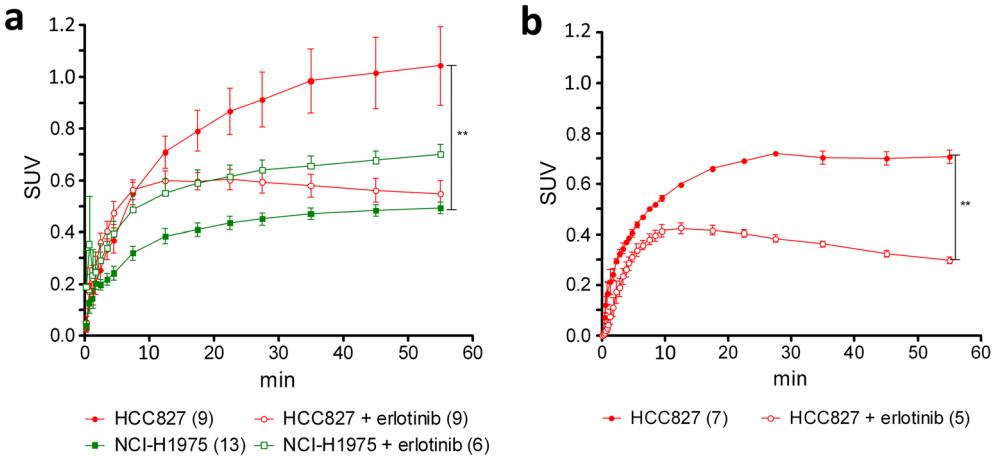

Fig. 4. Time-activity curves following i.v. injection of **a** 6-O-[^{18}F]FEE and **b** [^{11}C]erlotinib to NSCLC tumor–bearing mice with and without pre-injection of non-labeled erlotinib (6.4 ± 0.4 mg/kg). Results are presented as mean ± SEM, and the number of animals per group is listed in brackets. $^{**}p < 0.01$.

measured in HCC827 tumors (SUV ≅ 0.7) compared to NCI-H1975 and QG56 (SUV ≅ 0.2), at the same time point (Fig. 3) [20]. Moreover, 6-O-[^{18}F]FEE and [^{11}C]erlotinib exhibited accumulation and retention of radioactivity in HCC827 ($EGFR_m$) tumors, whereas a moderate washout of radioactivity from QG56 (wtEGFR) tumors was observed with time. Interestingly, however, the TACs of 6-O-[^{18}F]FEE and [^{11}C]erlotinib in NCI-H1975 tumors, which express both the p.L858R and the T790M mutation, presented different trends after the initial 10-min accumulation. Whereas [^{11}C]erlotinib was progressively cleared from these tumors, radioactivity levels had gradually increased in NCI-H1975 tumors after the injection of 6-O-[^{18}F]FEE.

To evaluate the extent of specific binding, erlotinib (6.4 mg/kg) was administered 3–10 min prior to the injection of 6-O-[^{18}F]FEE into HCC827 and NCI-H1975 tumor–bearing mice. As illustrated in Fig. 4, HCC827 SUV at 60 min had dropped by almost twofold compared to baseline (1.04 *vs.* 0.55), indicative of specific binding of 6-O-[^{18}F]FEE to the EGFR. Conversely, radioactivity levels measured in NCI-H1975 tumors were consistently higher with the administration of non-labeled erlotinib than

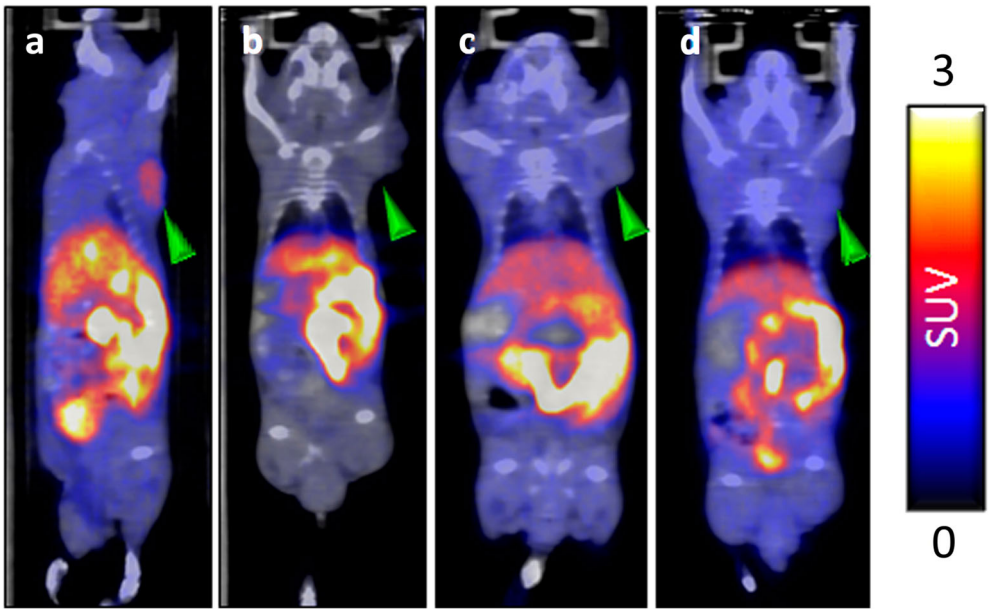

Fig. 5. Representative PET-CT coronal slice images following injection of 6-O-[^{18}F]FEE into **a** HCC827, **b** QG56, and **c** NCI-H1975 tumor–bearing mice. **d** Mouse is the same HCC827 tumor–bearing mouse presented in **a**, after pre-injection of non-labeled erlotinib (6.8 mg/kg). Tumors are indicated by the green arrowheads. Images are normalized to the same color scale and represent the summation of 30–60 min after 6-O-[^{18}F]FEE injection.

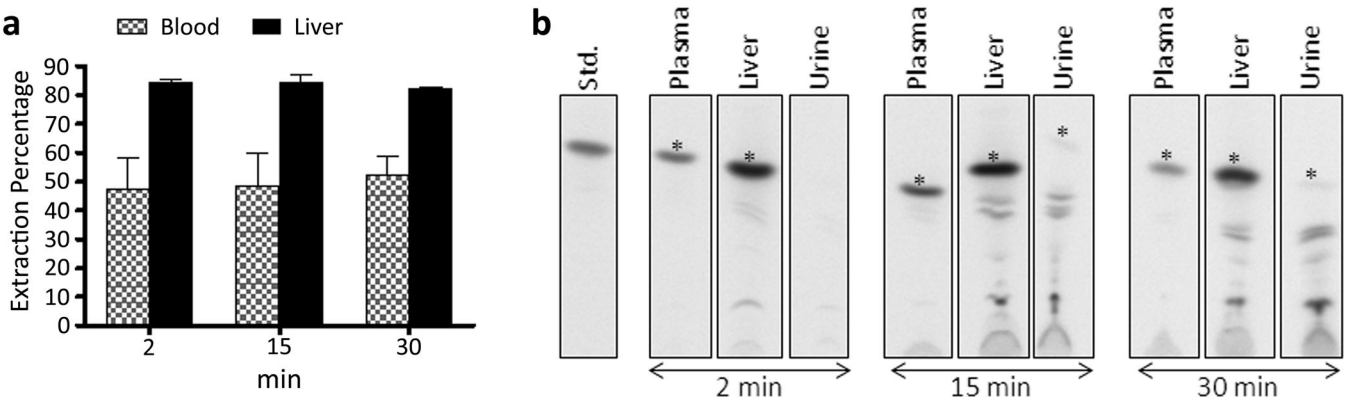

Fig. 6. **a** Extraction fractions of radioactivity from blood and liver samples following injection of 6-O-[^{18}F]FEE into BALB/c mice. **b** Representative radio-TLC images obtained after loading 6-O-[^{18}F]FEE standard (Std.), plasma, liver, and urine samples obtained at 2, 15, and 30 min after 6-O-[^{18}F]FEE injection. The band representing 6-O-[^{18}F]FEE in each sample is marked with an asterisk. Results are presented as mean ± SEM.

without. This suggested that the accumulation of 6-O-[^{18}F]FEE in NCI-H1975 tumors was principally non-specific and the higher radioactivity concentrations measured in NCI-H1975 tumors after administration of erlotinib in excess could most likely be attributed to the resulting higher radioactivity levels in blood, such as those reported for [^{11}C]erlotinib after the administration of non-labeled erlotinib in excess [32]. It should be noted that in our previous blocking studies, [^{11}C]erlotinib was *co-injected* with erlotinib (6.7 mg/kg) [20], whereas in the present study, erlotinib was administered *several minutes before* the injection of 6-O-[^{18}F]FEE, leading to the higher apparent radioactivity levels in HCC827 tumors during the first 5 min of the blocking experiment, compared to baseline (Fig. 4).

Since the presence of radioactive metabolites might also affect the measured SUVs and the extent of specific binding, the metabolic fate of 6-O-[^{18}F]FEE was investigated up to 30 min following its injection to mice. During this time, over 96 % of the radioactivity in plasma could be attributed to the intact compound, whereas radioactive metabolites were detected only in liver and urine samples, accounting for 15–20 % and 100 % of the radioactivity, respectively. Thus, the radioactive signal measured in NCI-H1975 tumors most likely results from non-specific binding of 6-O-[^{18}F]FEE, though it remains to be answered why, unlike in QG56 tumors, no washout of radioactivity from these tumors was observed with time. It is yet possible that part of 6-O-[^{18}F]FEE's binding to NCI-H1975 tumors is specific, but cannot be blocked with erlotinib. The two compounds could potentially exhibit different binding characteristics, such that 6-O-[^{18}F]FEE accumulation would be reduced after pre-administration of 6-O-FEE in excess, but not after erlotinib administration. This issue remains to be addressed in future studies.

Most patients with $EGFR_m$ tumors become resistant to erlotinib, gefitinib, or afatinib, with a PFS of 10–13 months. The EGFR T790M mutation, which is associated with acquired resistance to first- and second-line EGFR TKIs, has been reported in about 60 % of patients with disease progression after initial response to EGFR TKI therapy [6]. Such patients can still be treated with osimertinib, a third-generation irreversible EGFR TKI with activity against $EGFR_m$- and T790M-expressing NSCLC [37], which has also been recently approved for first-line treatment of $EGFR_m$ NSCLC [12]. Thus, the genetically diverse and dynamic molecular profile of NSCLC requires periodic monitoring for continuous optimization of therapy. Since not all patients with advanced NSCLC are suitable for (repeat) biopsy, alternative non-invasive approaches for examining EGFR's molecular status have been investigated, mostly focusing on liquid biopsies, such as circulating-free tumor DNA (ctDNA) and circulating tumor cells (CTCs). While the analysis of these circulating biomarkers from peripheral blood can potentially reveal spatial and temporal heterogeneity of tumors in real time, the paucity of tumor-associated markers with respect to other components in blood requires highly sensitive and specific isolation and detection technologies [38], posing a challenge on the clinical application of liquid biopsies. Although certain challenges concerning the clinical use of liquid biopsies remain, the cobas® EGFR Mutation Test v2 for analyzing ctDNA from plasma specimens of NSCLC patients has gained FDA approval in 2016, as a companion diagnostic test for identifying $EGFR_m$ NSCLC patients eligible for treatment with EGFR-targeted TKIs (https://www.fda.gov/drugs/informationondrugs/approveddrugs/ucm504540). Furthermore, in their recent guidelines, the College of American Pathologists, the International Association for the Study of Lung Cancer, and the Association for Molecular Pathology presented an expert consensus opinion supporting the use of ctDNA to identify T790M mutations in patients with progression or secondary resistance to EGFR-targeted TKIs [39].

Going forward, several questions remain to be addressed with respect to 6-O-[^{18}F]FEE, including its sensitivity and specificity in detecting the common activating mutations, as

well as uncommon EGFR mutations, which are found in about 10 % of NSCLC patients [7, 14] and resistance mutations, such as the secondary T790M mutation, MET amplification, or phenotype transformation. Interestingly, while our previously obtained results with [^{11}C]erlotinib suggest that tumors expressing the L858R and T790M mutations could be differentiated from those expressing the 746–750 (exon 19) ELREA deletion mutation or the L858R point mutation [20], Traxl and colleagues reported that the calculated distribution volume (V_T) of [^{11}C]erlotinib in NSCLC xenografts harboring an exon 19 deletion mutation was not different from those of resistant cells also expressing the T790M mutation or MET amplification [32]. In the current study, 6-O-[^{18}F]FEE could discriminate NSCLC xenografts with an $EGFR_m$ exon 19 deletion mutation from those bearing the wt receptor or a double-mutant (L858R + T790M) receptor. Its potential contribution to the precise molecular characterization of EGFR status in NSCLCs remains to be further investigated, particularly as a complementary diagnostic tool, *e.g.*, in cases of discordant results between tissue and liquid biopsies.

Finally, the semi-quantitative approach taken in the present study to analyze differences in tumor uptake may reflect only part of the full potential of 6-O-[^{18}F]FEE in discriminating and characterizing the mutational status of EGFR in NSCLCs. On the other end of the analytical scale, as the field of radiomics is increasingly applied in medical imaging [19], the radiomic PET signature of 6-O-[^{18}F]FEE could provide incremental value, rendering 6-O-[^{18}F]FEE - PET a useful surrogate and/or complementary screening tool for the stratification of NSCLC patients prior to and during EGFR TKI treatment and improving medical decision-making.

Conclusion

The fluorinated erlotinib analogue, 6-O-FEE, displays potency and selectivity characteristics towards various forms of the EGFR, which are similar to those of erlotinib. The results obtained following injection of 6-O-[^{18}F]FEE to NSCLC tumor–bearing mice illustrate that this radiopharmaceutical is capable of differentiating tumors harboring the wt receptor from those expressing an exon 19 deletion mutation or the double L858R + T790M mutations, warranting further clinical studies to characterize the full potential of this compound for PET MI of the EGFR in NSCLC patients.

Acknowledgements. The authors wish to thank the Cyclotron/Radiochemistry Unit's staff and Eng. Sassy Cohen in particular for their excellent technical support and assistance and the National Cancer Institute – the Division of Cancer Treatment and Diagnosis, Frederick, MD, USA, for providing the NCI-H3255 cell line.

Compliance with Ethical Standards. All animal studies were conducted under protocol number MD-13-13833-5, approved by the Animal Research Ethics Committee of the Hebrew University of Jerusalem, and in accordance with its guidelines.

Conflict of Interest

The authors declare that they have no conflict of interest.

References

1. Zhao D, Chen X, Qin N, Su D, Zhou L, Zhang Q, Li X, Zhang X, Jin M, Wang J (2017) The prognostic role of EGFR-TKIs for patients with advanced non-small cell lung cancer. Sci Rep 7:40374
2. Han SW, Kim TY, Hwang PG, Jeong S, Kim J, Choi IS, Oh DY, Kim JH, Kim DW, Chung DH, Im SA, Kim YT, Lee JS, Heo DS, Bang YJ, Kim NK (2005) Predictive and prognostic impact of epidermal growth factor receptor mutation in non-small-cell lung cancer patients treated with gefitinib. J Clin Oncol 23:2493–2501
3. Eberhard DA, Johnson BE, Amler LC, Goddard AD, Heldens SL, Herbst RS, Ince WL, Jänne PA, Januario T, Johnson DH, Klein P, Miller VA, Ostland MA, Ramies DA, Sebisanovic D, Stinson JA, Zhang YR, Seshagiri S, Hillan KJ (2005) Mutations in the epidermal growth factor receptor and in KRAS are predictive and prognostic indicators in patients with non-small-cell lung cancer treated with chemotherapy alone and in combination with erlotinib. J Clin Oncol 23:5900–5909
4. Mok T, Wu YL, Lee JS, Yu CJ, Sriuranpong V, Sandoval-Tan J, Ladrera G, Thongprasert S, Srimuninnimit V, Liao M, Zhu Y, Zhou C, Fuerte F, Margono B, Wen W, Tsai J, Truman M, Klughammer B, Shames DS, Wu L (2015) Detection and dynamic changes of EGFR mutations from circulating tumor DNA as a predictor of survival outcomes in NSCLC patients treated with first-line intercalated erlotinib and chemotherapy. Clin Cancer Res 21:3196–3203
5. Peled N, Roisman LC, Miron B, Pfeffer R, Lanman RB, Ilouze M, Dvir A, Soussan-Gutman L, Barlesi F, Tarcic G, Edelheit O, Gandara D, Elkabetz Y (2017) Subclonal therapy by two EGFR TKIs guided by sequential plasma cell-free DNA in EGFR-mutated lung cancer. J Thorac Oncol 12:e81–e84
6. (2017) NCCN Clinical Practice Guidelines in Oncology: https://www.nccn.org/professionals/physician_gls/default.aspx
7. Tan DS, Yom SS, Tsao MS et al (2016) The International Association for the Study of Lung Cancer Consensus Statement on Optimizing Management of EGFR Mutation-Positive Non-Small Cell Lung Cancer: status in 2016. J Thorac Oncol 11:946–963
8. Hirsch FR, Bunn PA Jr (2009) EGFR testing in lung cancer is ready for prime time. Lancet Oncol 10:432–433
9. Zhang YL, Yuan JQ, Wang KF, Fu XH, Han XR, Threapleton D, Yang ZY, Mao C, Tang JL (2016) The prevalence of EGFR mutation in patients with non-small cell lung cancer: a systematic review and meta-analysis. Oncotarget 7:78985–78993
10. Hanna N, Johnson D, Temin S, Baker S Jr, Brahmer J, Ellis PM, Giaccone G, Hesketh PJ, Jaiyesimi I, Leighl NB, Riely GJ, Schiller JH, Schneider BJ, Smith TJ, Tashbar J, Biermann WA, Masters G (2017) Systemic therapy for stage IV non-small-cell lung cancer: American Society of Clinical Oncology clinical practice guideline update. J Clin Oncol 35:3484–3515
11. Keedy VL, Temin S, Somerfield MR, Beasley MB, Johnson DH, McShane LM, Milton DT, Strawn JR, Wakelee HA, Giaccone G (2011) American Society of Clinical Oncology provisional clinical opinion: epidermal growth factor receptor (EGFR) mutation testing for patients with advanced non-small-cell lung cancer considering first-line EGFR tyrosine kinase inhibitor therapy. J Clin Oncol 29:2121–2127
12. US FDA approves TAGRISSO® (osimertinib) as 1st-line treatment for EGFR-mutated non-small cell lung cancer. https://www.astrazeneca.com/investor-relations/Stock-exchange-announcements/us-fda-approves-tagrisso-as-1st-line-treatment-for-egfr-mutated-non-small-cell-lung-cancer-19042018.html

13. Assi HI, Kamphorst AO, Moukalled NM, Ramalingam SS (2018) Immune checkpoint inhibitors in advanced non-small cell lung cancer. Cancer 124:248–261
14. Lindeman NI, Cagle PT, Beasley MB, Chitale DA, Dacic S, Giaccone G, Jenkins RB, Kwiatkowski DJ, Saldivar JS, Squire J, Thunnissen E, Ladanyi M (2013) Molecular testing guideline for selection of lung cancer patients for EGFR and ALK tyrosine kinase inhibitors: guideline from the College of American Pathologists, International Association for the Study of Lung Cancer, and Association for Molecular Pathology. J Thorac Oncol 8:823–859
15. Kris MG, Johnson BE, Berry LD, Kwiatkowski DJ, Iafrate AJ, Wistuba II, Varella-Garcia M, Franklin WA, Aronson SL, Su PF, Shyr Y, Camidge DR, Sequist LV, Glisson BS, Khuri FR, Garon EB, Pao W, Rudin C, Schiller J, Haura EB, Socinski M, Shirai K, Chen H, Giaccone G, Ladanyi M, Kugler K, Minna JD, Bunn PA (2014) Using multiplexed assays of oncogenic drivers in lung cancers to select targeted drugs. JAMA 311:1998–2006
16. Arcila ME, Oxnard GR, Nafa K, Riely GJ, Solomon SB, Zakowski MF, Kris MG, Pao W, Miller VA, Ladanyi M (2011) Rebiopsy of lung cancer patients with acquired resistance to EGFR inhibitors and enhanced detection of the T790M mutation using a locked nucleic acid-based assay. Clin Cancer Res 17:1169–1180
17. Rachiglio AM, Esposito Abate R, Sacco A, Pasquale R, Fenizia F, Lambiase M, Morabito A, Montanino A, Rocco G, Romano C, Nappi A, Iaffaioli RV, Tatangelo F, Botti G, Ciardiello F, Maiello MR, de Luca A, Normanno N (2016) Limits and potential of targeted sequencing analysis of liquid biopsy in patients with lung and colon carcinoma. Oncotarget 7:66595–66605
18. Sacher AG, Paweletz C, Dahlberg SE, Alden RS, O'Connell A, Feeney N, Mach SL, Jänne PA, Oxnard GR (2016) Prospective validation of rapid plasma genotyping for the detection of EGFR and KRAS mutations in advanced lung cancer. JAMA Oncol 2:1014–1022
19. Liu Y, Kim J, Balagurunathan Y et al (2016) Radiomic features are associated with EGFR mutation status in lung adenocarcinomas. Clin Lung Cancer 17:441–448 e446
20. Abourbeh G, Itamar B, Salnikov O et al (2015) Identifying erlotinib-sensitive non-small cell lung carcinoma tumors in mice using [^{11}C]erlotinib PET. EJNMMI Res 5:4. https://doi.org/10.1186/s13550-014-0080-0
21. Slobbe P, Windhorst AD, Stigter-van Walsum M et al (2015) A comparative PET imaging study with the reversible and irreversible EGFR tyrosine kinase inhibitors [^{11}C]erlotinib and [^{18}F]afatinib in lung cancer-bearing mice. EJNMMI Res 5:14. https://doi.org/10.1186/s13550-015-0088-0
22. Huang S, Han Y, Chen M, Hu K, Qi Y, Sun P, Wang M, Wu H, Li G, Wang Q, du Z, Zhang K, Zhao S, Zheng X (2018) Radiosynthesis and biological evaluation of ^{18}F-labeled 4-anilinoquinazoline derivative (^{18}F-FEA-Erlotinib) as a potential EGFR PET agent. Bioorg Med Chem Lett 28:1143–1148
23. Jain A, Kameswaran M, Pandey U, Prabhash K, Sarma HD, Dash A (2017) ^{68}Ga labeled Erlotinib: a novel PET probe for imaging EGFR over-expressing tumors. Bioorg Med Chem Lett 27:4552–4557
24. Fenizia F, De Luca A, Pasquale R et al (2015) EGFR mutations in lung cancer: from tissue testing to liquid biopsy. Future Oncol 11:1611–1623
25. Slobbe P, Poot AJ, Windhorst AD, van Dongen GAMS (2012) PET imaging with small-molecule tyrosine kinase inhibitors: TKI-PET. Drug Discov Today 17:1175–1187
26. van Dongen GA, Poot AJ, Vugts DJ (2012) PET imaging with radiolabeled antibodies and tyrosine kinase inhibitors: immuno-PET and TKI-PET. Tumour Biol 33:607–615
27. Bahce I, Yaqub M, Errami H et al (2016) Effects of erlotinib therapy on [^{11}C]erlotinib uptake in EGFR mutated, advanced NSCLC. EJNMMI Res 6:10. https://doi.org/10.1186/s13550-016-0169-8
28. Memon AA, Weber B, Winterdahl M, Jakobsen S, Meldgaard P, Madsen HHT, Keiding S, Nexo E, Sorensen BS (2011) PET imaging of patients with non-small cell lung cancer employing an EGF receptor targeting drug as tracer. Br J Cancer 105:1850–1855
29. Petrulli JR, Sullivan JM, Zheng M-Q, Bennett DC, Charest J, Huang Y, Morris ED, Contessa JN (2013) Quantitative analysis of [^{11}C]-erlotinib PET demonstrates specific binding for activating mutations of the EGFR kinase domain. Neoplasia 15:1347–1353
30. Weber B, Winterdahl M, Memon A, Sorensen BS, Keiding S, Sorensen L, Nexo E, Meldgaard P (2011) Erlotinib accumulation in brain metastases from non-small cell lung cancer: visualization by positron emission tomography in a patient harboring a mutation in the epidermal growth factor receptor. J Thorac Oncol 6:1287–1289
31. Bahce I, Smit EF, Lubberink M, van der Veldt AAM, Yaqub M, Windhorst AD, Schuit RC, Thunnissen E, Heideman DAM, Postmus PE, Lammertsma AA, Hendrikse NH (2013) Development of [^{11}C]erlotinib positron emission tomography for in vivo evaluation of EGF receptor mutational status. Clin Cancer Res 19:183–193
32. Traxl A, Beikbaghban T, Wanek T, Kryeziu K, Pirker C, Mairinger S, Stanek J, Filip T, Sauberer M, Kuntner C, Berger W, Langer O (2017) [^{11}C]Erlotinib PET cannot detect acquired erlotinib resistance in NSCLC tumor xenografts in mice. Nucl Med Biol 52:7–15
33. Rodnick ME, Brooks AF, Hockley BG, Henderson BD, Scott PJH (2013) A fully-automated one-pot synthesis of [^{18}F]fluoromethylcholine with reduced dimethylaminoethanol contamination via [^{18}F]fluoromethyl tosylate. Appl Radiat Isot 78:26–32
34. Dent MF, Hubbold L, Radford H, Wilson AP (1995) The methylene blue colorimetric microassay for determining cell line response to growth factors. Cytotechnology 17:27–33
35. Petrulli JR, Hansen SB, Abourbeh G, Yaqub M, Bahce I, Holden D, Huang Y, Nabulsi NB, Contessa JN, Mishani E, Lammertsma AA, Morris ED (2017) A multi species evaluation of the radiation dosimetry of [^{11}C]erlotinib, the radiolabeled analog of a clinically utilized tyrosine kinase inhibitor. Nucl Med Biol 47:56–61
36. Carey KD, Garton AJ, Romero MS, Kahler J, Thomson S, Ross S, Park F, Haley JD, Gibson N, Sliwkowski MX (2006) Kinetic analysis of epidermal growth factor receptor somatic mutant proteins shows increased sensitivity to the epidermal growth factor receptor tyrosine kinase inhibitor, erlotinib. Cancer Res 66:8163–8171
37. Passaro A, Guerini-Rocco E, Pochesci A, Vacirca D, Spitaleri G, Catania CM, Rappa A, Barberis M, de Marinis F (2017) Targeting EGFR T790M mutation in NSCLC: from biology to evaluation and treatment. Pharmacol Res 117:406–415
38. Lim M, Kim CJ, Sunkara V, Kim MH, Cho YK (2018) Liquid biopsy in lung cancer: clinical applications of circulating biomarkers (CTCs and ctDNA). Micromachines 9. https://doi.org/10.3390/mi9030100
39. Lindeman NI, Cagle PT, Aisner DL, Arcila ME, Beasley MB, Bernicker EH, Colasacco C, Dacic S, Hirsch FR, Kerr K, Kwiatkowski DJ, Ladanyi M, Nowak JA, Sholl L, Temple-Smolkin R, Solomon B, Souter LH, Thunnissen E, Tsao MS, Ventura CB, Wynes MW, Yatabe Y (2018) Updated molecular testing guideline for the selection of lung cancer patients for treatment with targeted tyrosine kinase inhibitors: guideline from the College of American Pathologists, the International Association for the Study of Lung Cancer, and the Association for Molecular Pathology. Arch Pathol Lab Med 142:321–346
40. Mock BH, Winkle W, Vavrek MT (1997) A color spot test for the detection of Kryptofix 2.2.2 in [^{18}F]FDG preparations. Nucl Med Biol 24:193–195